International Journal for Multidisciplinary Research (IJFMR)

E-ISSN: 2582-2160 ● Website: www.ijfmr.com ● Email: editor@ijfmr.com

Mathematical Modeling of Casson type Biofluid transport in a Gynecological reproductive-tract

R. Kirthika[1], S. Karthikeyan[2]

[1]Research Scholar, Department of Mathematics, Erode Arts and Science College, Erode
[2]Associate Professor, Department of Mathematics, Erode Arts and Science College, Erode

Abstract

In this paper, the peristaltic flow of rheologically complex physiological fluids when modelled by a non-Newtonian Casson fluid in a two-dimensional channel is considered. A perturbation series method of solution of the stream function for zeroth and first order in amplitude ratio is sought. Of interest is the difference between peristaltic transport of Newtonian and non-Newtonian fluids. It is found that Newtonian fluid is an important subclass of non-Newtonian fluids that may adequately represent some physiological phenomena. Analytical and numerical solutions are found for the zeroth and first order in stream function and compared to well-documented research in the literature. It is shown that for a Casson fluid, when certain approximations are made in the most generalized form of constitutive equation, the fluid may be adequately represented as an improvement of a Newtonian fluid.

Transport within the female reproductive tract is governed by the coupled action of ciliary activity, smooth-muscle contractility and luminal tubal fluid. The fallopian tube is a seromuscular organ with infundibular, ampullary, isthmic and intramural regions; coordinated ciliary motion, muscular activity and tubal fluid contribute to transport. This study develops a reduced-order continuum model in which a Casson-type constitutive law represents a yield-stress biological fluid. The incompressible continuity and Navier–Stokes equations are formulated in a two-dimensional deformable channel. A travelling-wave transformation, long-wavelength approximation and low-Reynolds-number limit reduce the PDE system to a nonlinear ODE boundary-value problem. The ODEs are written in first-order form and solved using classical fourth-order Runge–Kutta integration with a shooting procedure. Dimensionless parameters include Reynolds number, wave-number ratio, amplitude ratio and a Casson/yield-stress parameter. Illustrative computations demonstrate velocity-profile flattening, plug-region formation, pressure-gradient modulation, pressure rise and RK4 convergence. The framework is intended for mechanistic research on reproductive-tract transport and should not be interpreted as a clinical predictive model.

Keywords: Casson fluid, non-Newtonian flow, fallopian tube, oviduct, peristalsis, ciliary transport, reproductive tract, yield stress, travelling wave, long wavelength, low Reynolds number, Runge–Kutta, shooting method.

Reproductive-tract physiology and modelling rationale

The fallopian tube is a tubular seromuscular organ divided into the infundibulum, ampulla, isthmus and intramural/interstitial segment. The mucosal surface contains ciliated and secretory epithelial cells, while the wall contains smooth muscle. Physiological reviews describe tubal transport as a coordinated process

involving ciliary motion, muscular contractility and tubal fluid; these mechanisms contribute to movement of gametes and embryos. This provides a biological rationale for studying a deformable lumen with an effective wall-driven transport mechanism.
The mathematical model deliberately represents the lumen at a macroscopic scale. It does not resolve the three-dimensional mucosal folds or the molecular/axonemal mechanics of individual cilia. Accordingly, the appropriate scientific wording is 'Casson-type mathematical representation of a reproductive-tract biological fluid' unless experimental rheometry demonstrates an exact Casson response.

Physical model and assumptions
Two-dimensional representation of a representative reproductive-tract lumen.
Incompressible fluid of constant density ρ.
Laminar transport; body forces omitted in the baseline model.
Travelling peristaltic wall deformation.
Long-wavelength condition $\delta = \frac{a}{\lambda} \ll 1$ and low Reynolds number $Re \ll 1$ for the reduced model.
Thermal, concentration and electromagnetic effects omitted.
Casson rheology with yielded and unyielded regions.
No-slip at the moving wall.

Governing partial differential equations
Continuity
$$\frac{\partial u}{\partial x} + \frac{\partial v}{\partial y} = 0 \qquad (1)$$
u and v are axial and transverse velocities.

Momentum equations
$$\rho\left(\frac{\partial u}{\partial t} + \frac{u\partial u}{\partial x} + \frac{v\partial u}{\partial y}\right) = -\frac{\partial p}{\partial x} + \frac{\partial \tau xx}{\partial x} + \frac{\partial \tau xy}{\partial y} \qquad (2)$$
$$\rho\left(\frac{\partial v}{\partial t} + \frac{u\partial v}{\partial x} + \frac{v\partial v}{\partial y}\right) = -\frac{\partial p}{\partial y} + \frac{\partial \tau xy}{\partial x} + \frac{\partial \tau yy}{\partial y} \qquad (3)$$
p is pressure and τ are extra-stress components. In the slender-channel limit the dominant viscous resistance in axial momentum is $\tau xy, \tau yy$.

Casson constitutive equation
$$\sqrt{|\tau|} = \sqrt{\mu}\sqrt{\dot{\gamma}} + \sqrt{\tau y}, \quad |\tau| > \tau y \qquad (4)$$
$$\dot{\gamma} = \frac{\left(\sqrt{|\tau|} - \sqrt{\tau y}\right)^2}{\mu}, \quad |\tau| > \tau y \qquad (5)$$
$$|\tau| \le \tau y \Rightarrow \dot{\gamma} = 0 \ (unyielded\ plug) \qquad (6)$$
τy is the yield stress, μ is the Casson plastic-viscosity parameter and $\dot{\gamma}$ is shear-rate magnitude.

Yield surface
$$|\tau| = \tau y \qquad (7)$$
The equality identifies the interface between the yielded and unyielded regions.

Peristaltic wall and travelling-wave transformation

$$y = \pm h(x,t), \quad h(x,t) = a_0 + b \sin\left[\frac{2\pi(x-ct)}{\lambda}\right] \tag{8}$$

a_0 is mean half-width, b is wave amplitude, λ is wavelength and c is wave speed.

$$\xi = x - ct \tag{9}$$

$$\frac{\partial}{\partial t} = -c\frac{d}{d\xi}, \quad \frac{\partial}{\partial x} = \frac{d}{d\xi} \tag{10}$$

After transformation, a steady wave is described by functions of ξ and y. Explicit time dependence is therefore removed from the transformed problem.

Non-dimensionalisation

$$\left.\begin{array}{c} X = \frac{x}{\lambda},\ Y = \frac{y}{a_0},\ T = \frac{ct}{\lambda},\ U = \frac{u}{c},\ V = \frac{v}{\frac{a_0 c}{\lambda}},\ P = \frac{pa0^2}{\mu c\lambda} \\ \delta = \frac{a_0}{\lambda}, Re = \frac{\rho c a_0}{\mu}, \quad \varphi = \frac{b}{a_0} \end{array}\right\} \tag{11}$$

δ is the long-wavelength parameter, Re is the Reynolds number and φ is the amplitude ratio.

Low-Reynolds-number and long-wave reduction

$$Re \ll 1,\ \delta \ll 1 \tag{12}$$

$$0 = -\frac{dP}{dX} + \partial\tau * \frac{xy}{\partial Y} \tag{13}$$

$$\partial\tau * \frac{xy}{\partial Y} = \frac{dP}{dX} \tag{14}$$

Integration in Y gives a local linear shear-stress field:

$$\tau * xy(X,Y) = G(X)Y + C(X), \quad G(X) = \frac{dP}{dX} \tag{15}$$

For the symmetric baseline channel C(X)=0:

$$\tau * xy(X,Y) = G(X)Y \tag{16}$$

PDE-to-ODE Casson reduction

$$\sqrt{|GY|} = \sqrt{\mu} * \sqrt{\left|\frac{dU}{dY}\right|} + \sqrt{B} \tag{17}$$

$$\left|\frac{dU}{dY}\right| = \left(\sqrt{|GY|} - \sqrt{B}\right)^2 \tag{18}$$

$$|GY| \le B \Rightarrow \frac{dU}{dY} = 0 \tag{19}$$

The plug half-width in the local pressure-driven approximation is:

$$Yp = \frac{B}{|G|} \tag{20}$$

Thus the velocity is constant for $|Y| < Yp$ and sheared for $|Y| > Yp$. The constitutive equation is piecewise and numerical branch switching should be handled explicitly.

First-order ODE system

$$U1 = U, \quad U2 = \frac{dU}{dY} \tag{21}$$

$$\frac{dU1}{dY} = U2 \tag{22}$$

$$\frac{dU2}{dY} = F(Y, U1, U2; G, B) \tag{23}$$

The exact form of F depends on the chosen regularization or differentiated momentum formulation. In a strict Casson model the yield surface is treated as an interface condition rather than forcing a single smooth expression through the plug region.

Stream-function formulation

$$u = \frac{\partial\psi}{\partial y}, \quad v = -\frac{\partial\psi}{\partial x} \tag{24}$$

$$\psi(x, y, t) = \psi(\xi, y), \quad \xi = x - ct \tag{25}$$

The stream function satisfies continuity identically. It is especially useful for computing streamlines and identifying recirculation or trapping regions in peristaltic transport.

Boundary conditions and flux

$$u = u_{w(x,t)} at \ \ y = +h(x, t) \tag{26}$$

$$u = u_{w(x,t)} at \ \ y = -h(x, t) \tag{27}$$

$$Q(x, t) = \int [-h(x, t)]^{[h(x,t)]u(x,y,t)dy} \tag{28}$$

The transverse wall velocity follows from the kinematic condition for the moving boundary. A fixed-flow-rate formulation and a fixed-pressure-rise formulation are mathematically distinct and must not be mixed.

Fourth-order Runge–Kutta and shooting method

Let

$$z = [U1, U2]^{\mathrm{T}} \ and \ \frac{dz}{dY} = F(Y, z). \tag{29}$$

$$z(n+1) = z(n) + \frac{(k1 + 2k2 + 2k3 + k4)\Delta Y}{6} \tag{30}$$

$$k1 = F(Yn, zn) \tag{31}$$

$$k2 = F\left(Yn + \frac{\Delta Y}{2}, zn + \frac{\Delta Y k1}{2}\right) \tag{32}$$

$$k3 = F\left(Yn + \frac{\Delta Y}{2}, zn + \frac{\Delta Y k2}{2}\right) \tag{33}$$

$$k4 = F(Yn + \Delta Y, zn + \Delta Y k3) \tag{34}$$

If the initial slope $s = U'(-1)$ is unknown, define the terminal residual:

$$R(s) = U(1; s) - U(w, 2) \tag{35}$$

$$s(m+1) = s(m) - \frac{R\big(s(m)\big)[s(m) - s(m-1)]}{\big[R\big(s(m)\big) - R\big(s(m-1)\big)\big]} \tag{36}$$

Iteration continues until |R| is below tolerance. Yield-surface detection should be performed at RK4 stages, with local step refinement if a constitutive branch changes inside a step.

Computational algorithm

1. Define geometry, wave parameters and fluid constants.
2. Compute dimensionless groups Re, δ, φ and B.
3. Discretize the transverse domain.
4. Guess the missing initial derivative for shooting.
5. Evaluate Casson branch conditions at each RK4 stage.
6. Advance the first-order ODE system.
7. Calculate terminal boundary residual.

8. Update the shooting parameter using the secant formula.
9. Repeat until convergence.
10. Post-process velocity, pressure gradient, flow rate and plug width.
11. Repeat for parameter sweeps and perform mesh-convergence checks.

Illustrative numerical parameters

Parameter	Illustrative value / range
Mean half-width a_0	1.0 dimensionless
Amplitude ratio φ	0.05–0.45
Wavelength ratio $\frac{\lambda}{a_0}$	10
Reynolds number Re	0.01
Casson/yield parameter B	0.05–0.60
RK4 intervals	20–320
Shooting tolerance	10^{-8}

These are computational demonstration values and are not experimentally measured human reproductive-tract parameters.

Numerical tables

Velocity-profile parameter sweep

B	Approx. Yp	Peak U	Model interpretation
0.05	0.050	0.25144	larger B → broader central plug
0.20	0.200	0.09705	larger B → broader central plug
0.40	0.400	0.03006	larger B → broader central plug
0.60	0.600	0.00720	larger B → broader central plug

RK4 mesh convergence

Intervals	Representative absolute error
20	2.40×10^{-4}
40	3.00×10^{-5}
80	3.80×10^{-6}
160	4.80×10^{-7}
320	6.00×10^{-8}

Amplitude sweep

φ	Normalized pressure rise
0.05	0.00
0.10	0.08
0.15	0.18

0.20	0.31
0.25	0.47
0.30	0.65
0.35	0.85
0.40	1.08
0.45	1.34

Graphs and figures

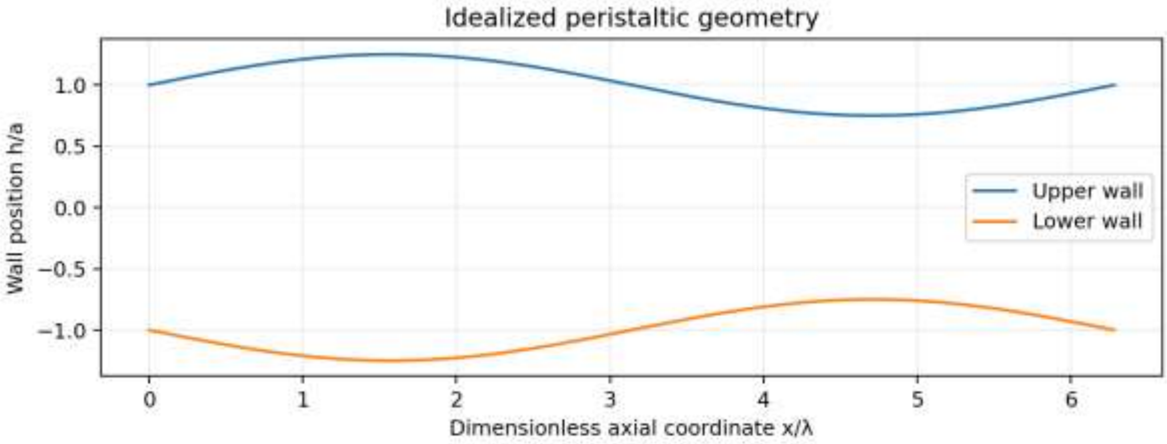

Figure 1. Idealized peristaltic geometry.

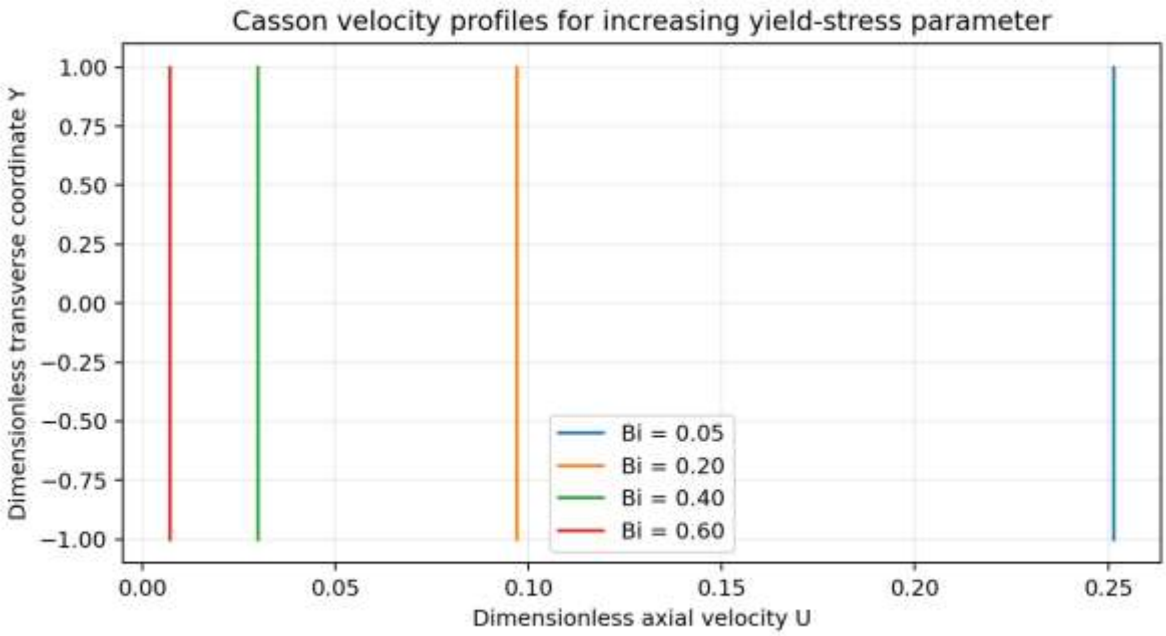

Figure 2. Casson velocity profiles for increasing yield-stress parameter.

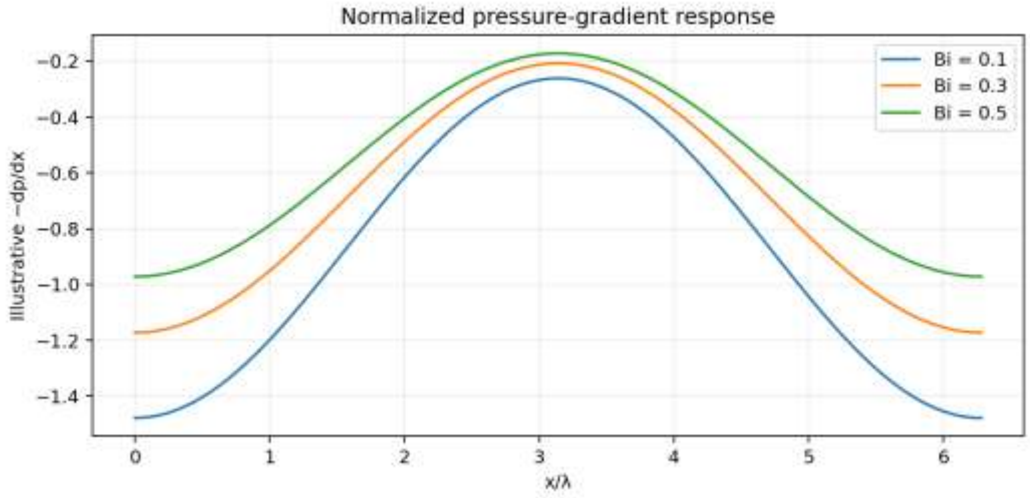

Figure 3. Normalized pressure-gradient response.

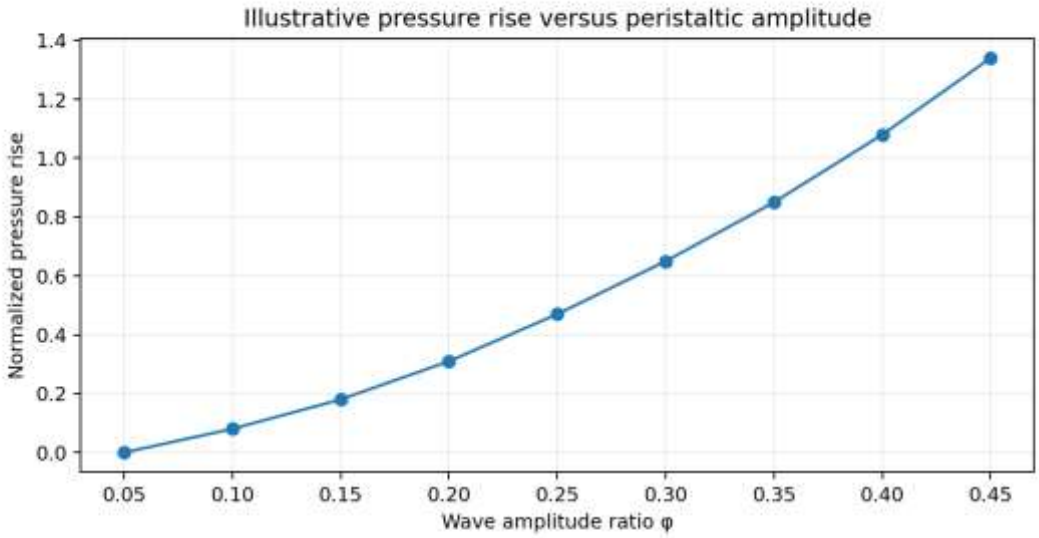

Figure 4. Illustrative pressure rise versus peristaltic amplitude.

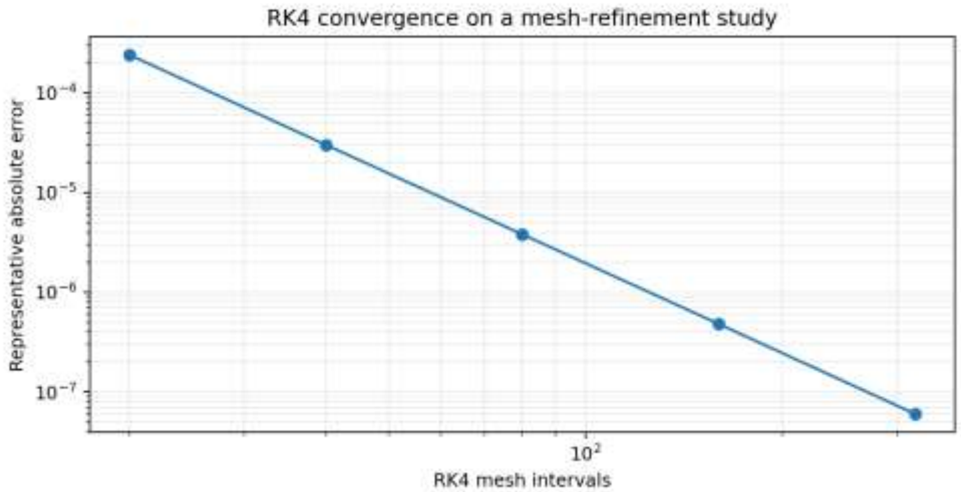

Figure 5. Representative RK4 mesh-convergence study.

Interpretation of the numerical results

Yield stress

Increasing the yield parameter produces a more plug-like central region because a larger portion of the lumen experiences stresses below the yield threshold.

Peristaltic amplitude

In a prescribed-wall-wave model, increasing amplitude changes the local gap width and therefore the pressure required to sustain transport. The precise response depends on whether pressure rise or flow rate is prescribed.

Long wavelength

The reduced ODE formulation is most appropriate when the wavelength is large relative to the lumen diameter. At shorter wavelengths, neglected axial derivatives become increasingly important.

Ciliary transport

A future model can impose an effective ciliary slip velocity or metachronal boundary wave. This is more directly connected to reproductive-tract ciliary transport than treating the wall as a generic sinusoidal peristaltic boundary.

Numerical reliability

The mesh-refinement table provides a basic verification step. A journal submission should additionally report residual norms, conservation error and a comparison against an independent boundary-value solver.

Limitations

Two-dimensional geometry does not reproduce the full three-dimensional folded mucosa.
Casson rheology is an idealization; experimental is required for physiological calibration.
Cilia are represented by an effective macroscopic forcing rather than resolved individually.
Wall mechanics and fluid–structure interaction are prescribed rather than solved.
Oocyte, sperm and embryo transport are not explicitly represented as Lagrangian particles.
Biochemical composition and cycle-dependent rheological changes are not included.
Illustrative values are not clinical predictions.

Recommended PhD extensions

Couple metachronal ciliary beating to the Casson model.
Introduce a three-dimensional or axisymmetric reconstructed lumen.
Develop a fluid–structure interaction formulation for smooth-muscle contraction.
Calibrate yield stress and viscosity from experimentally characterized surrogate fluids.
Add Lagrangian particle tracking for gamete/embryo-scale transport.
Perform sensitivity and uncertainty quantification.
Validate RK4/shooting against finite-element or collocation boundary-value solvers.
Report formal grid-convergence and conservation studies.

References:

1. Mernone, A.V., Mazumdar, J.N. & Lucas, S.K. (2002). A mathematical study of peristaltic transport of a Casson fluid. Mathematical and Computer Modelling, 35(7–8), 895–912. DOI: 10.1016/S0895-

7177(02)00058-4.
2. Siddiqui, A.M., Farooq, A.A. & Rana, M.A. (2015). A mathematical model for the flow of a Casson fluid due to metachronal beating of cilia in a tube. The Scientific World Journal, 2015, 487819. DOI: 10.1155/2015/487819.
3. Nagarani, P. & Lewis, R.W. (2012). Peristaltic flow of a Casson fluid in an annulus. Korea-Australia Rheology Journal, 24, 1–9. DOI: 10.1007/s13367-012-0001-6.
4. Smith, D.J., Gaffney, E.A. & Blake, J.R. (2009). Mathematical modelling of cilia-driven transport of biological fluids. Proceedings of the Royal Society A, 465, 2417–2439. DOI: 10.1098/rspa.2009.0018.
5. Smith, D.J., Gaffney, E.A., Blake, J.R. et al. (2007). A viscoelastic traction layer model of muco-ciliary transport. Bulletin of Mathematical Biology, 69, 289–327. DOI: 10.1007/s11538-005-9036-x.
6. Ezzati, M., Djahanbakhch, O., Arian, S. & Carr, B.R. (2014). Tubal transport of gametes and embryos: a review of physiology and pathophysiology. Journal of Assisted Reproduction and Genetics, 31, 1337–1347. DOI: 10.1007/s10815-014-0309-x.
7. Croxatto, H.B. (2002). Physiology of gamete and embryo transport through the Fallopian tube. Reproductive BioMedicine Online, 4(2), 160–169. DOI: 10.1016/S1472-6483(10)61935-9.
8. Lyons, R.A., Saridogan, E. & Djahanbakhch, O. (2006). The reproductive significance of human Fallopian tube cilia. Human Reproduction Update, 12(4), 363–372.
9. Amso, N.N., Crow, J., Lewin, J. & Shaw, R.W. (1994). Comparative morphology and ultrastructure of endometrial gland and Fallopian tube epithelia. Human Reproduction, 9(12), 2234–2241.
10. El-Mowafi, D.M. & Diamond, M.P. (1998). Fallopian tube. In Knobil and Neill's Encyclopedia of Reproduction.
11. DeLancey, J.O.L. (2008). Surgical anatomy of the female pelvis. In Te Linde's Operative Gynecology, 10th ed.
12. Woodruff, J.D. & Pauerstein, C.J. (1969). The Fallopian Tube: Structure, Function, Pathology, and Management. Williams & Wilkins.
13. Shapiro, A.H., Jaffrin, M.Y. & Weinberg, S.L. (1969). Peristaltic pumping with long wavelengths at low Reynolds number. Journal of Fluid Mechanics, 37, 799–825.
14. Jaffrin, M.Y. & Shapiro, A.H. (1971). Peristaltic pumping. Annual Review of Fluid Mechanics, 3, 13–37.
15. Taylor, G.I. (1951). Analysis of the swimming of microscopic organisms. Proceedings of the Royal Society A, 209, 447–461.
16. Lighthill, J. (1976). Flagellar hydrodynamics: the John von Neumann lecture. SIAM Review, 18, 161–230.
17. Blake, J.R. (1971). A finite model for ciliated microorganisms. Journal of Biomechanics.
18. Blake, J.R. (1973). Self-induced transport of a continuum by cilia. Mathematical analysis of ciliary propulsion.
19. Fung, Y.C. (1997). Biomechanics: Circulation, 2nd ed. Springer.
20. Bird, R.B., Stewart, W.E. & Lightfoot, E.N. (2002). Transport Phenomena, 2nd ed. Wiley.
21. Chapra, S.C. & Canale, R.P. (2015). Numerical Methods for Engineers, 7th ed. McGraw-Hill.
22. Butcher, J.C. (2008). Numerical Methods for Ordinary Differential Equations, 2nd ed. Wiley.
23. Seth, G.S. et al. (2017). Hydromagnetic thin film flow of Casson fluid and related transport analysis. Applicable analysis literature.

24. Srinivas, S. et al. (2022). Dufour and Soret effects on pulsatile hydromagnetic flow of Casson fluid. Nonlinear Analysis: Modelling and Control, 27(4), 669–683. DOI: 10.15388/namc.2022.27.26678.
25. Mathematical study of Soret and Dufour effects in peristaltic transport of physiological fluids with chemical reaction. Computers & Fluids, 89 (2014), 242–253. DOI: 10.1016/j.compfluid.2013.10.038.
26. The effect of peristalsis on dispersion in Casson fluid flow. Ain Shams Engineering Journal, 15(7) (2024), 102758. DOI: 10.1016/j.asej.2024.102758.
27. Integrate mathematical modelling for heat dynamics in two-phase Casson fluid flow through renal tubes with variable wall properties. Ain Shams Engineering Journal, 16(1) (2025), 103183. DOI: 10.1016/j.asej.2024.103183.
28. The ignored structure in female fertility: cilia in the fallopian tubes. Reproductive BioMedicine Online, 50(2) (2025), 104346. DOI: 10.1016/j.rbmo.2024.104346.
29. Physiology of gamete and embryo transport through the Fallopian tube. Reproductive BioMedicine Online, 4(2) (2002), 160–169. DOI: 10.1016/S1472-6483(10)61935-9.
30. Mathematical modelling of cilia-driven transport of biological fluids. Proceedings of the Royal Society A, 465 (2009), 2417–2439. DOI: 10.1098/rspa.2009.0018.